

AperTO - Archivio Istituzionale Open Access dell'Università di Torino

Gate crashing arbuscular mycorrhizas: in vivo imaging shows the extensive colonization of both symbionts by *Trichoderma atroviride*

This is a pre print version of the following article:

Original Citation:

Availability:

This version is available <http://hdl.handle.net/2318/149629> since 2016-05-30T07:56:16Z

Published version:

DOI:10.1111/1758-2229.12221

Terms of use:

Open Access

Anyone can freely access the full text of works made available as "Open Access". Works made available under a Creative Commons license can be used according to the terms and conditions of said license. Use of all other works requires consent of the right holder (author or publisher) if not exempted from copyright protection by the applicable law.

(Article begins on next page)



UNIVERSITÀ DEGLI STUDI DI TORINO

This is an author version of the contribution published on:

Questa è la versione dell'autore dell'opera:

[ENVIRONMENTAL MICROBIOLOGY REPORTS, DOI: 10.1111/1758-2229.12221]

The definitive version is available at:

La versione definitiva è disponibile alla URL:

[<http://onlinelibrary.wiley.com/doi/10.1111/1758-2229.12221/abstract>]

Gate crashing arbuscular mycorrhizas: *in vivo* imaging shows the extensive colonization of both symbionts by *Trichoderma atroviride*

Beatrice Lace¹, Andrea Genre¹, Sheridan Woo², A. Faccio³, Matteo Lorito² & Paola Bonfante¹

¹Department of Life Science and Systems Biology, Università degli Studi di Torino, Viale Mattioli 25-10125 Torino, Italy;

²Department of Agriculture, Università degli Studi di Napoli Federico II

³Institute of Sustainable Plant Protection, CNR, Torino

Corresponding author: Paola Bonfante; Telephone: +00390116502927; Fax: +00390116705962; E-mail: paola.bonfante@unito.it

SUMMARY

Plant growth promoting fungi include strains of *Trichoderma* species that are used in biocontrol, and arbuscular mycorrhizal (AM) fungi, that enhance plant nutrition and stress resistance. The concurrent interaction of plants with these two groups of fungi affects crop performance, but has only been occasionally studied so far. Using *in vivo* imaging of GFP-tagged lines, we investigated the cellular interactions occurring between *Trichoderma atroviride* PKI1, *Medicago truncatula* and two *Gigaspora* species under *in vitro* culture conditions. *T. atroviride* did not activate symbiotic-like responses in the plant cells, such as nuclear calcium spiking or cytoplasmic aggregations at hyphal contact sites. Furthermore, *T. atroviride* parasitized *G. gigantea* and *G. margarita* hyphae through localized wall breaking and degradation - although this was not associated with significant chitin lysis nor the upregulation of two major chitinase genes. *T. atroviride* colonized broad areas of the root epidermis, in association with localized cell death. The infection of both symbionts was

This article has been accepted for publication and undergone full peer review but has not been through the copyediting, typesetting, pagination and proofreading process, which may lead to differences between this version and the Version of Record. Please cite this article as doi: 10.1111/1758-2229.12221

This article is protected by copyright. All rights reserved.

24 also observed when *T. atroviride* was applied to a pre-established AM symbiosis. We conclude that
25 – although this triple interaction is known to improve plant growth in agricultural environments – in
26 vitro culture brings to light a strong mycoparasitic potential for a biocontrol strain of *Trichoderma*.

28 INTRODUCTION

29 The release of plant root exudates in the rhizosphere attracts a multitude of microbes that thrive in
30 this nutrient-rich niche. In addition to obligate biotrophs, like arbuscular mycorrhizal (AM) fungi
31 belonging to Glomeromycota, the rhizosphere also hosts many facultative saprotrophic fungi.
32 *Trichoderma/Hypocrea* spp. are present in soil, litter, dead wood, and are commonly isolated from
33 the rhizosphere at all soil depths (Harman *et al.*, 2004). These fungi successfully exploit a multitude
34 of substrates, supported by their large arsenal of poly- and oligo-saccharide hydrolytic enzymes
35 (Druzhinina *et al.*, 2012). In particular, chitinases and glucanases allow *Trichoderma* species to act
36 as mycotrophs that antagonize, parasitize and kill other fungi. This feature has made the genus
37 *Trichoderma* a first-choice in biocontrol against fungal pathogens (Harman *et al.*, 2004), with the
38 most common biocontrol strains belonging to *T. harzianum*, *T. asperellum/asperelloides*, *T.*
39 *hamatum*, *T. viride* and *T. atroviride* (Druzhinina *et al.*, 2012). In addition, the direct interaction
40 with root cells can trigger plant induced systemic resistance, another mechanism of disease control,
41 (Harman *et al.*, 2004). Evidence indicates that the association of *Trichoderma* species with plant
42 roots can range from symbiosis (Lorito and Woo, 2014) to endophytism and facultative
43 pathogenicity (Druzhinina *et al.*, 2012), and involves the exploitation of plant derived carbohydrates
44 by the fungus (Vargas *et al.*, 2009). Altogether, *Trichoderma* strains are more and more used as
45 biofertilizers for their ability to stimulate plant growth (Harman, 2011) and defenses (Palmieri *et*
46 *al.*, 2012). Recently, several molecular determinants for such capabilities have been identified
47 following the genomic and transcriptomic analyses of *T. reesei* (Martinez *et al.*, 2008), *T. virens*
48 and *T. atroviride* (Kubicek *et al.*, 2011; Atanasova *et al.*, 2013).

When growing in the rhizosphere or on root surface, *Trichoderma* is expected to have frequent interactions with plant mutualistic symbionts such as AM fungi (Bonfante and Genre, 2010). Indeed, such interactions have been investigated in the past, but - depending on the experimental setup - the inoculation with both fungi either resulted in positive synergistic effects on plant health or the inhibition of plant growth (Chandanie *et al.*, 2009; Rousseau *et al.*, 1996). Furthermore, *T. harzianum* has displayed mycoparasitic activity on *Rhizophagus* sp. inside alginate beads (De Jeager *et al.*, 2011). In order to fine tune effective biological control strategies that exploit these beneficial rhizospheric fungi, a more thorough understanding of their complex interaction and relationship with the plants is required.

In this work, an *in vitro* method already established to monitor the early phases of the interaction between *Medicago truncatula* and *Gigaspora gigantea* (Genre *et al.*, 2005; 2008; 2009) was extended to a triple system by adding a GFP-tagged strain of *Trichoderma atroviride* biocontrol isolate PKI1. We investigated the dual interaction between the two fungi and observed a mycoparasitic activity of the biocontrol agent, noticing that *T. atroviride* equally colonizes live and UV-killed AM hyphae; our results also indicate that mycoparasitism is not associated with extensive chitin lysis and two major *T. atroviride* chitinase genes (ECH42 and NAG1) are not significantly upregulated. Analyzing the dual interaction between *T. atroviride* and *M. truncatula*, we observed extensive hyphal colonization of root cells, associated with localized cell death; furthermore, *T. atroviride* PKI1 did not trigger plant symbiotic responses such as the activation of nuclear calcium spiking (Singh and Parniske, 2012) or prepenetration-associated cytoplasmic aggregations at hyphal contact sites (Genre *et al.*, 2005; 2007). Lastly, by studying the triple interaction between *T. atroviride*, *G. gigantea* and *M. truncatula*, we concluded that the symbiotic condition does not protect the plant nor the glomeromycete from *T. atroviride* infection.

RESULTS

Trichoderma atroviride PKI1 parasitizes *Gigaspora gigantea*

75 When grown in dual interaction (see Materials and methods in Supplemental File 7 for a full
76 description of the experimental setup) *T. atroviride* PKI1 and *G. gigantea* hyphae were clearly
77 visualized and distinguishable in both stereo- and confocal microscopy, thanks to the constitutive
78 green fluorescence of the GFP-tagged *T. atroviride* PKI1 mycelium and the strong autofluorescence
79 of *G. gigantea* (Figure 1). Hyphae of *T. atroviride* were 4-5 μm in diameter, septate, in contrast to
80 the larger (around 10 μm), aseptate hyphae of *G. gigantea*. Occasional septa could be spotted
81 delimiting terminal hyphal section devoid of cytoplasm, as often observed in Glomeromycota
82 hyphae arising from spore germination in the absence of a host plant. The first contacts between *G.*
83 *gigantea* and *T. atroviride* hyphae (growing without apparent tropism) were observed 24 hours
84 post-inoculation (hpi) as presented in Figure 1A. None of the specialized hyphal structures typically
85 developed by *Trichoderma* during mycoparasitic and non-mycoparasitic interactions, such as
86 coiling filaments or appressoria (Lu *et al.*, 2004), were observed at this time.

87 Transmission electron microscopy visualized the wall ultrastructure of both fungi at sites of hyphal
88 contact. The wall was more electron-transparent in *T. atroviride* than *G. gigantea*, which displayed
89 two distinct electron-dense layers and localized amorphous extrusions (Figures 2A and 2B).

90 At 48 hpi, *Trichoderma* deployed a widespread, highly branched mycelium, intermingling and
91 overlapping the sparser *G. gigantea* hyphae. At this time, *T. atroviride* had penetrated and grown
92 inside several hyphae of the glomeromycete (Figures 1B and 1C). Outbursts of the parasitized
93 hypha cytoplasm were clearly visible around the perforation points (Figure 1B). Remarkably, *T.*
94 *atroviride* hyphae formed clusters of short branches inside the extruded cytoplasm, protruding
95 towards the damaged AM mycelium. Intra-hyphal growth of *T. atroviride* proceeded rapidly,
96 possibly facilitated by the absence of septa (Figure 1C). Seventy-two hpi, *T. atroviride* had
97 extensively colonized the inside of several *G. gigantea* hyphae, and wrapped around the
98 glomeromycete auxiliary cells with short, convoluted hyphae (Figures 1D and 1E).

99 Transmission electron microscopy revealed that hyphal penetration sites were associated with a
100 structural damage of the *G. gigantea* wall (Figure 2C): breaking points were observed in areas

101 where the inner electron-dense layer was reduced to a loose fibrillar network, although the outer
102 amorphous extrusions showed no evident sign of degradation (Figure 2D). Importantly, the
103 glomeromycete cytoplasm was reduced to a degenerated clump with no recognizable inner
104 structure. Comparable senescence events in the AM fungus were never observed in control plates of
105 the same age (Supplemental Figures 1A and 1B). By contrast, the mycoparasite hyphae displayed
106 an active cytoplasm, very rich in organelles (Figure 2C).

107 Beside timing the phases of the *T. atroviride* / *G. gigantea* interaction, our combined confocal and
108 electron microscopy observations demonstrate that *T. atroviride* can effectively mycoparasitize an
109 AM fungus when grown in axenic dual cultures, with a major degradation of the glomeromycete
110 cytoplasm and intense, local dismantling of the wall texture in the parasitized hyphae.

112 ***T. atroviride* mycoparasitism is not associated with major chitinolytic activity**

113 In order to assess whether local wall degradation was associated with chitin lysis by *T. atroviride*
114 chitinases, we performed a cytochemical detection of chitin by applying gold-labelled wheat germ-
115 agglutinin, a lectin that specifically binds chitin (Bonfante *et al.*, 1990) on electron microscopy
116 samples. As expected, both *Trichoderma atroviride* and *Gigaspora gigantea* cell walls resulted to
117 be homogeneously labelled (Supplemental Figure 2). However, quantitative image analysis did not
118 reveal any statistical difference in the gold granule amount between uncolonized and parasitized
119 AM hyphae (Supplemental Figure 2D). This suggests that the observed wall dismantling does not
120 significantly impact the chitin component.

121 This finding was further confirmed by experiments with two strains of *T. atroviride* expressing a
122 cytoplasmic GFP under either the 42-kDa endochitinase promoter (*ech42::gfp*) or the β -N-
123 acetylglucosaminidase promoter (*nag1::gfp*). Both promoters are known to be activated when
124 *Trichoderma* is grown in the presence of chitin as its major carbon source (Carsolio *et al.*, 1999;
125 Brunner *et al.*, 2003). When the two strains were grown in the presence of *G. gigantea*, the timing

126 and pattern of their infection process was the same as for PKI1. Fluorescence quantification showed
127 no relevant change in the expression of *ech42* (endochitinase) during the whole time-course of the
128 experiment, compared to the control; *nag1* (exochitinase) expression level was only weakly
129 enhanced 24 hours post *T. atroviride* inoculation (earlier than the first hyphal contacts) and
130 decreased to values lower than the control at 96 hpi, when contacts and mycoparasitic colonization
131 were observed (see Supplemental Figures 3A and 3B).

132 The observation that two major chitinases of *T. atroviride* (an endo- and an exochitinase) were not
133 significantly upregulated during the parasitic phase indirectly supports the results of wall chitin
134 labelling experiments, suggesting that chitin lysis in the parasitized hyphal wall has not a major role
135 in the mycoparasitic event.

136

137 ***Trichoderma atroviride* mycoparasitism does not require viable host hyphae**

138 To better understand whether the observed extensive hyphal colonization involves any active
139 response by the AM fungus, the glomeromycete hyphae (*G. margarita*), was exposed to 90 min UV
140 irradiation prior to inoculation of *T. atroviride*. The effective loss of viability in the AM hyphae was
141 assessed by confocal microscopy observations, which revealed the stop of all cytoplasmic streams
142 (see Supplemental Movies 4 and 5). Importantly, no outbreak of cytoplasm was observed,
143 indicating that *G. margarita* cell walls were intact. As in the previous experiments, the two fungi
144 were clearly recognizable due to their distinct fluorescence wavelengths (Figure 3). The time-course
145 of the interaction was exactly the same as in the presence of the viable AM fungus. *Trichoderma*
146 could be spotted inside *Gigaspora* hyphae starting from 48 hpi (Figures 3A and 3B); massive
147 colonization sites were marked by multiple coiled hyphae completely filling the AM hyphal lumen
148 (Figure 3A).

149 Interestingly, observations at 72 hpi showed *Trichoderma* preferentially growing in *Gigaspora*
150 cytoplasm-filled hyphae, while avoiding empty hyphal branches (Figure 3C). A time-lapse
151 sequence is shown in Figures 3D-3I (and Supplemental Movie 6), showing a *Trichoderma* hypha

152 proceeding all along a *Gigaspora* hypha and branching in correspondence of the parasitized hyphal
153 branches. Subsequent profuse branching led to the occupation of most of the hyphal lumen (Figure
154 3H). The swelling of *Trichoderma* hyphal tip was evident as it reached the apex of the *Gigaspora*
155 hypha (Figure 3H). Eventually, *T. atroviride* exited the *G. margarita* apex by perforating its
156 terminal wall (Figure 3I).

157 These observations showed that *T. atroviride* is able to colonize both viable and non-viable AM
158 hyphae, pointing out that no active response or signaling from *Gigaspora* is required to elicit the
159 mycoparasitic process. In spite of its wide array of chitinolytic enzymes, *T. atroviride* preferentially
160 grew in cytoplasm-filled hyphae. This suggests that *G. margarita* cytoplasm represents a more
161 convenient substrate compared to the chitinous cell wall.

162

163 ***M. truncatula* root colonization by *T. atroviride* in dual cultures is associated with localized cell** 164 **death**

165 We used *M. truncatula* root organ cultures expressing the GFP-HDEL marker for the endoplasmic
166 reticulum (ER) to assess plant cell viability and cytoplasm reorganization (Genre *et al.*, 2009)
167 during the dual interaction with *T. atroviride*. Twenty-four hours post inoculation, the fungus had
168 grown diffusely, forming highly branched hyphae that extended radially from the inoculum plug
169 (data not shown). At 48 hpi, isolated hyphae approached *M. truncatula* roots, but no direct contact
170 was observed yet (Figure 4A). At this stage, root epidermal and cortical cells displayed a regular
171 lace-like network of GFP-labelled ER cisternae, not different from control roots, indicating that
172 hyphal vicinity did not affect cell viability (Figure 4B and Supplemental Figure 1D). At 72 hpi, the
173 mycelium had almost entirely covered the Petri dish. Confocal microscopy revealed that the
174 mycelium had extensively contacted the root epidermis (Figure 4C), but appressorium-like
175 structures or root penetration events were never observed. Nevertheless, a partial disruption of the
176 ER tubular structure was evident in epidermal and cortical cells, as GFP fluorescence was reduced
177 to separate puncta and patches (Figure 4D). Cytoplasmic aggregations, typically observed in the

178 same experimental system upon contact with glomeromycetes or biotrophic pathogenic fungi
179 (Genre *et al.*, 2009), were never detected in the presence of *T. atroviride*. 144 hours post *T.*
180 *atroviride* inoculation (6 days), the GFP-HDEL fluorescence had disappeared from all epidermal
181 cells, indicating a significant loss of viability. As shown in Figure 4E and 4F, the cell borders were
182 only marked by the reddish wall autofluorescence that in lively roots is covered by the bright GFP
183 signal. The appearance of diffuse GFP fluorescence in the lumen of a few cells (Figure 4E and 4F)
184 was likely due to more severe disruption of endocellular membranes. At this stage, single optical
185 sections acquired from root inner focal planes revealed the presence of *T. atroviride* within the root
186 tissues, growing inside the lumen of dead cells (Figure 4F). Control *M. truncatula* root cultures of
187 the same age displayed a healthy ER with no cell death or other evident sign of senescence (see
188 Supplemental Figures 1C and 1D).

189 These observations indicate that in our experimental conditions *T. atroviride* PKI1 acts as an
190 endophytic root colonizer, causing localized cell death. Importantly, fungal contacts with the root
191 epidermis do not trigger any of the pre-penetration cell responses typically observed during
192 symbiotic or biotrophic pathogenic interactions: the formation of ER patches inside cytoplasmic
193 aggregations at contact sites (Genre *et al.*, 2009) was in fact never observed.

194

195 ***T. atroviride* culture filtrates do not induce nuclear calcium signals in *M. truncatula***

196 We therefore decided to further investigate whether *T. atroviride* could activate early symbiotic
197 responses in *M. truncatula*. A central element in the legume perception of both glomeromycetes and
198 rhizobia is the so-called common symbiotic signaling pathway, or CSSP (Singh and Parniske,
199 2012). Its activation triggers persistent nuclear calcium oscillations known as calcium spiking
200 (Sieberer *et al.*, 2009; Chabaud *et al.*, 2011). *T. atroviride* culture filtrates have previously been
201 shown to activate defense-related responses (characteristic calcium signals and programmed cell
202 death) in cells of soybean (Navazio *et al.*, 2007). On this basis, we applied an analogous *T.*
203 *atroviride* culture filtrate to *M. truncatula* roots expressing the calcium-sensitive NUP-YC2.1

204 probe. Filtrates were obtained from *T. atroviride* cultures grown on either liquid M medium or
205 sterile water: none of them triggered any variation in the nuclear calcium level of epidermal cells.
206 As a positive control we used culture filtrates from *Gigaspora margarita*, which elicited intense
207 nuclear calcium spiking, as expected (Chabaud *et al.*, 2011). Representative calcium plots are
208 shown in Figure 5.

209 We conclude that *T. atroviride* exudates do not activate the CSSP in *M. truncatula* ROCs,
210 suggesting that the plant is not perceiving *Trichoderma* diffusible signals through this conserved
211 symbiotic pathway.

212

213 **Root and hyphal colonization by *T. atroviride* is not influenced by the AM symbiotic status**

214 In order to investigate the effect of *T. atroviride* on the symbiotic interaction *M. truncatula* / *G.*
215 *gigantea*, mycorrhizal co-cultures were allowed to develop for 15 days before the inoculation with
216 *T. atroviride*. AM establishment was monitored daily under a stereomicroscope and eventually
217 confirmed by confocal microscopy. Root epidermal cells contacted by *G. gigantea* hyphae and
218 hyphopodia displayed a healthy ER network, fully comparable to uninoculated control roots (Figure
219 6A). Similarly, intracellular hyphae were observed in healthy epidermal and cortical cells (Figure
220 6B). Lastly, several inner cortical cells contained fully developed arbuscules, confirming the active
221 status of the symbiosis (as displayed in Figure 6C). *T. atroviride* developed profusely as early as 24
222 hpi, similarly to what was observed in the dual interaction experiments described above. Forty-
223 eight hours post *T. atroviride* inoculation, no direct contact was occurring and both *M. truncatula*
224 epidermal cells and *G. gigantea* hyphae displayed a healthy aspect, fully comparable to controls
225 (Figures 7A and 7B). *T. atroviride* hyphae spread over the root surface at 72 hpi and proliferated
226 with particular intensity in the vicinity of *G. gigantea* (Figure 7C): branches and coils were
227 observed at this stage around *G. gigantea* auxiliary cells (Figure 7D). Following contact with *T.*
228 *atroviride*, several root cells had lost their GFP-HDEL fluorescence (Figure 7D). After 144 hours (6
229 days) the mycelium of *T. atroviride* had entirely covered the medium surface. Dense hyphal coils

230 had developed inside some of the auxiliary cells of *G. gigantea*, entirely filling their lumen (Figure
231 7F) and causing the loss of cytoplasmic autofluorescence (and, on that account, viability). Areas of
232 epidermal cell death could be observed throughout the root system, which were almost completely
233 void of GFP-HDEL fluorescence (Figure 7E). In accordance with our observations of dual
234 interaction, penetration and coiling of *T. atroviride* hyphae inside the cortical cells of *M. truncatula*
235 root was also detected (Figures 7G and 7H). Synchronous observation of control plates lacking *T.*
236 *atroviride* inoculation showed that the active status of the AM mycorrhization persisted throughout
237 the experimental period. In this case, the lace-like structure of the ER in *M. truncatula* epidermal
238 cells, as well as the *G. gigantea* autofluorescence, were fully maintained (Supplemental Figures 1E
239 and 1F), indicating no loss of viability for either symbiont.

240 Altogether, the development of *T. atroviride* infection, at least in terms of microscopic morphology,
241 was not affected by the symbiotic status of the *M. truncatula* / *G. gigantea* interaction. The
242 mycoparasite colonized *M. truncatula* roots, leading to localized cell death, and penetrated *G.*
243 *gigantea* hyphae and auxiliary cells, thus affecting the viability of the AM fungus. In conclusion,
244 the development of *T. atroviride* was fully comparable in the mycorrhizal (triple) and non-
245 mycorrhizal (dual) interactions.

246

247 DISCUSSION

248 *T. atroviride* dismantles glomeromycetes wall and feeds on their cytoplasm

249 In our experimental conditions, *T. atroviride* PKI1 penetrated *G. gigantea* and *G. margarita* hyphae
250 with localized cell wall dismantling, in analogy to the process described for other species of
251 *Trichoderma* parasitizing the AM fungus *Rhizophagus irregularis* or several phytopathogens
252 (Benhamou and Chet, 1997; Rousseau *et al.*, 1996). Such processes have long been ascribed to the
253 action of cell wall degrading enzymes - chitinases, glucanases and proteases - and secondary
254 metabolites (Di Pietro *et al.*, 1993; Lorito *et al.*, 1993a; 1993b; 1994; 1996; Schirmböck *et al.*,
255 1994; Zeilinger *et al.*, 1999). This was supported by targeted gene knock-out or overexpression

256 experiments (Woo *et al.*, 1999; Djonović *et al.*, 2006; Djonović *et al.*, 2007) and genome
257 sequencing of a few *Trichoderma* species (Martinez *et al.*, 2008; Kubicek *et al.*, 2011), where a
258 huge inventory of genes encoding poly- and oligosaccharide hydrolytic enzymes has been found
259 (Druzhinina *et al.*, 2012). Nevertheless, a genome-wide expression study has indicated that *T.*
260 *atroviride* mostly expresses glucanases belonging to the GH16 family and proteases during
261 *Rhizoctonia solani* colonization (Atanasova *et al.*, 2013), suggesting that chitinases are not major
262 determinants of mycoparasitism in this species. Our results are in line with this view and show that
263 *T. atroviride* can enter the complex multilayered wall of a Gigasporacean AM fungus – reportedly
264 composed of chitin, beta 1-4 glucans, mannans and proteins (Bonfante, 2001; Tisserant *et al.*,
265 2013). Nevertheless, the dismantling of the glomeromycete cell wall was only evident at penetration
266 sites, in the immediate vicinity of intra-hyphal hyphae. Wall degradation mainly involved the
267 electron dense components of the wall, exposing a loose fibrillar network, probably representing the
268 untouched chitin skeleton. This appears to be sufficient to grant wall loosening and access of the
269 mycoparasite to the coenocytic hyphal lumen. The fact that both major chitinases of *T. atroviride*
270 were not upregulated during its interaction with the AM fungus - as highlighted by our experiments
271 with *ech42::gfp* and *nag1::gfp* strains - indirectly supports this hypothesis.

272 Furthermore, our experiments with UV-killed *Gigaspora margarita* show that *T. atroviride* does
273 not require any active response by the glomeromycete to start its colonization. Moreover, the
274 colonization of living AM fungal hyphae followed exactly the same timing and pattern, suggesting
275 that AM hyphae are prone to *T. atroviride* mycoparasitism.

276

277 ***T. atroviride* causes root cell death**

278 *Trichoderma* spp. are free-living fungi, widespread in soil and root ecosystems, but selected strains
279 are widely used in agriculture because of their beneficial effect on plant stress response and yield.
280 This led to the description of *Trichoderma* species as beneficial - or even symbiotic - plant growth

281 promoters (Harman, 2000; 2011; Harman *et al.*, 2004; Chacon *et al.*, 2007). However local cellular
282 and molecular responses to *Trichoderma* colonization are not fully understood or, in the case of *T.*
283 *atroviride*, completely unknown.

284 Our live observation of *T. atroviride* / *M. truncatula* interaction shows that *T. atroviride* exudates
285 do not trigger typical symbiotic responses such as the activation of the CSSP pathway or the
286 assembly of cytoplasmic aggregations at hyphal contact sites (Genre *et al.*, 2005; 2009). In contrast
287 with this early stealth approach, *T. atroviride* causes localized plant cell death within six days post
288 inoculation - similarly to what has been described upon the attack by the necrotrophic fungus
289 *Phoma medicaginis* (Genre *et al.*, 2009). Such cell death responses, including programmed cell
290 death and leading to the formation of necrotic areas, have sometimes been observed, although not
291 fully characterized, in several *Trichoderma*-treated plants at root and seed surface (Howell, 2006
292 and Howell C. personal communication). Significantly, such responses are more evident when the
293 interaction is established *in vitro*, on sugar-rich substrates, or when the secreted metabolites are
294 used instead of the living fungus (Navazio *et al.*, 2007). It is a common understanding that, under
295 natural conditions, local root lesions caused by these beneficial microbes are indeed tolerated by the
296 plant. Necrotic lesions have been proposed to be necessary for achieving the “priming” effect, by
297 which several *Trichoderma* strains activate plant defense responses to ‘true’ pathogens (Brotman *et*
298 *al.*, 2012; 2013; Tucci *et al.*, 2011; Palmieri *et al.*, 2012). Similarly, Deshmukh *et al.* (2006)
299 demonstrated that the endophyte *Piriformospora indica*, known to promote growth on a broad
300 spectrum of host plants (Schäfer *et al.*, 2007), also requires cells death for its successful
301 proliferation in differentiated barley roots.

302 Recent studies have demonstrated the extensive “reprogramming” of host plant physiology
303 following the establishment of a successful root colonization by effective *Trichoderma* strains, as
304 noted on both the expressome and the proteome (Harman, 2011; Lorito *et al.*, 2010; Morán-Diez *et*

305 *al.*, 2012; Shores *et al.*, 2010; Perazzoli *et al.*, 2012). A targeted gene expression study on plant
306 cell death markers should finally demonstrate if (programmed) cell death is a necessary step at least
307 in some plant-*Trichoderma* interactions to activate systemic resistance or growth promotion
308 responses. For sure, the contrast is striking with the root colonization mechanism in AM, where the
309 preservation of plant cell integrity is required for fungal penetration and symbiosis establishment
310 (Bonfante and Genre, 2010).

311

312 **Arbuscular mycorrhiza does not alleviate *T. atroviride*-induced damage on either *M.***
313 ***truncatula* or *G. gigantea***

314 DeJaeger *et al.* (2010) studied the mycoparasitic interaction between *T. harzianum* and *G.*
315 *intraradices*, and reported that intraradical AM mycelium colonizing potato roots was susceptible to
316 *T. harzianum* invasion. In their experimental conditions, the presence of the AM fungus seems to be
317 required for root penetration by *T. harzianum*, with no apparent detrimental effects on either the
318 plant or the AM fungus. By contrast, our results show that *T. atroviride* can directly colonize root
319 tissues - regardless of the presence of an AM fungus - and affect the viability of both *G. gigantea*
320 hyphae and *M. truncatula* root cells. Furthermore, confocal microscopy never showed the presence
321 of *T. atroviride* inside the intraradical mycelium of *G. gigantea*, in apparent contradiction with the
322 hypothesis that *Trichoderma* spp. exploit the glomeromycete mycelium as an access route to inner
323 root tissues. This contrasting evidence could be due to the different fungal and plant species, as well
324 as to the high level of adaptability of these ecologically successful root-associated microbes. In fact,
325 DeJaeger and colleagues (2010) had purposely chosen a strain of *T. harzianum* known for its
326 inability to penetrate the roots of *S. tuberosum*, in order to highlight the intraradical AM mycelium-
327 mediated colonization mechanism. It should also be noted that our experimental setup imposes the
328 use of root organ cultures lacking the aerial part of the plant. As a consequence, systemic and
329 physiological responses due to the combined action of the two fungi (Martínez-Medina *et al.*, 2011)

could not be taken into account. We cannot exclude that *in vitro* conditions gave *Trichoderma* a particularly favourable environment to deploy its mycoparasitic and plant necrotrophic strategies. Further studies can now be envisaged to assess the importance of these phenomena in natural conditions, where the complexity and competitiveness of the rhizosperic environment may mitigate the aggressiveness that *Trichoderma* displayed in our *in vitro* conditions.

In conclusion, a combination of detailed live imaging, electron microscopy studies and live gene expression analyses of the interactions between a biocontrol strain of *Trichoderma* and plant/fungal AM partners, revealed several unexpected features, providing novel clues for the understanding of such complex interactions. In this line, our cell-biology based results nicely complement the recent transcriptomic data produced after *Trichoderma* genome sequencing.

Acknowledgments

The authors express their thank to Dr. R. W. Roberson, (SOLS, Arizona State University) for advices on electron microscopy fixation protocols and to Dr. M. Novero for her assistance with statistical analyses. Research was funded by MIUR-PRIN 2008 project to PB and ML.

BL performed all experiments, analyzed the data and contributed to the writing; AG performed confocal microscopy experiments, analyzed the data and contributed to the writing; AF performed the electron microscopy experiments; SW and ML analyzed the data and contributed to the writing; PB conceived the experimental design; analyzed the data and wrote the manuscript.

LITERATURE CITED

Atanasova L., Le Crom S., Gruber S., Coulpier F., Seidl-Seiboth V., Kubicek C. P. and Druzhinina I. P. 2013. Comparative transcriptomics reveals different strategies of *Trichoderma* mycoparasitism. BMC Genomics 14, 121.

355
 356 Bécard, G. and Fortin, J.A. 1988. Early events of vesicular-arbuscular mycorrhiza formation on Ri
 357 T-DNA transformed roots. *New Phytol.* 108, 211–18.
 358
 359 Benhamou, N. and Chet, I. 1997. Cellular and molecular mechanisms involved in the interaction
 360 between *Trichoderma harzianum* and *Pythium ultimum*. *Appl. Environ. Microbiol.* 63, 2095–2099.
 361
 362 Boisson-Dernier, A., Chabaud, M., Garcia, F., Bécard, G., Rosenberg, C., Barker, DG. 2001.
 363 *Agrobacterium rhizogenes*-transformed roots of *Medicago truncatula* for the study of nitrogen-
 364 fixing and endomycorrhizal symbiotic associations. *MPMI* 14, 695–700.
 365
 366 Bonfante, P., Vian, B., Perotto, S., Faccio, A., Knox, J.P. 1990. Cellulose and pectin localization in
 367 roots of mycorrhizal *Allium porrum*: labelling continuity between host cell wall and interfacial
 368 material. *Planta* 180, 537–547.
 369
 370 Bonfante, P. 2001. At the interface between mycorrhizal fungi and plants: the structural
 371 organization of cell wall, plasma membrane and cytoskeleton. In: Hock B (ed) *The Mycota IX.*
 372 *Fungal associations.* Springer, Berlin, 45–91.
 373
 374 Bonfante, P. & Genre, A. 2010. Mechanisms underlying beneficial plant-fungus interactions in
 375 mycorrhizal symbiosis. *Nat commun.* 1, 48.
 376

377 Brotman, Y., Lisec, J., Méret, M., Chet, I., Willmitzer, L., Viterbo, A. 2012. Transcript and
 378 metabolite analysis of the *Trichoderma*-induced systemic resistance response to *Pseudomonas*
 379 *syringae* in *Arabidopsis thaliana*. *Microbiology* 22, 139–146.

380

381 Brotman, Y., Landau, U., Cuadros-Inostroza, Á., Takayuki, T., Fernie, A.R., *et al.* 2013.
 382 *Trichoderma*-plant root colonization: escaping early plant defense responses and activation of the
 383 antioxidant machinery for saline stress tolerance. *PLoS Pathog* 9(3): e1003221.

384

385 Brunner, K., Peterbauer, C. K., Mach, R. L., Lorito, M., Zeilinger, S., Kubicek, C. P. 2003. The
 386 Nag1 *N*-acetylglucosaminidase of *Trichoderma atroviride* is essential for chitinase induction by
 387 chitin and of major relevance to biocontrol. *Curr. Genet.* 43, 289-295.

388

389 Carsolio, C., Benhamou, N., Haran, S., Cortés, C., Gutiérrez, A., Chet, I., Herrera-Estrella, A.
 390 1999. Role of the *Trichoderma harzianum* endochitinase gene, *ech42*, in mycoparasitism. *Appl.*
 391 *Environ. Microbiol.* 65, 929-935.

392

393 Chabaud, M., Venard, C. & Barker, D. G. 2002. Targeted inoculation of *Medicago truncatula* in
 394 vitro root cultures reveals MtENOD11 expression during early stages of infection by
 395 arbuscular mycorrhizal fungi. *New Phytol.*, 156, 265–273.

396

397 Chabaud, M., Genre, A., Sieberer, B. J., Faccio, A., Fournier, J., Novero, M., Barker, D.G.,
 398 Bonfante, P. 2011. Arbuscular mycorrhizal hyphopodia and germinated spore exudates trigger Ca^{2+}

399 spiking in the legume and nonlegume root epidermis. *New Phytol* 189, 347-55.

400

401 Chacon, M.R., Rodríguez-Galán, O., Benítez, T., Sousa, S., Rey, M., Llobell, A., Delgado-Jarana,

402 J. 2007. Microscopic and transcriptome analyses of early colonization of tomato roots by

403 *Trichoderma harzianum*. *Int. Microbiol* 10,19–27.

404

405 Chandanie, W.A., Kubota, M., Hyakumachi, M. 2009. Interactions between the arbuscular

406 mycorrhizal fungus *Glomus mosseae* and plant growth-promoting fungi and their significance for

407 enhancing plant growth and suppressing damping-off of cucumber (*Cucumis sativus* L.). *App Soil*

408 *Ecol* 41, 336-341.

409

410 De Jaeger, N., Declerck, S., De la Providencia, I. E. 2010. Mycoparasitism of arbuscular

411 mycorrhizal fungi: a pathway for the entry of saprotrophic fungi into roots. *FEMS microbiol ecolol*

412 73, 312–22.

413

414 De Jaeger, N., de la Providencia, I. E., Rouhier, H., Declerck, S. 2011. Co-entrapment of

415 *Trichoderma harzianum* and *Glomus sp.* within alginate beads: impact on the arbuscular

416 mycorrhizal fungi life cycle. *J Appl microbiol* 111, 125–35.

417

418 Deshmukh, S., Hückelhoven, R., Schäfer, P., Imani, J., Sharma, M., Weiss, M., Waller, F., Kogel,

419 K.H. 2006. The root endophytic fungus *Piriformospora indica* requires host cell death for

420 proliferation during mutualistic symbiosis with barley. *PNAS* 103, 18450-7.

421

422 Di Pietro A., Lorito, M., Hayes, C.K., Broadway R.M. and Harman, G.E. 1993. Endochitinase from
423 *Gliocladium virens*: isolation, characterization and synergistic antifungal activity in combination
424 with gliotoxin. *Phytopathology* 83, 308-313.

425

426 Djonović, S., Pozo, M.J., Kenerley, C.M. 2006. Tvbg3, a beta-1,6-glucanase from the biocontrol
427 fungus *Trichoderma virens*, is involved in mycoparasitism and control of *Pythium ultimum*. *Appl*
428 *Environ Microbiol.* 72, 7661-70.

429

430 Djonović, S., Vittone, G., Mendoza-Herrera, A., Kenerley, C.M. 2007. Enhanced biocontrol
431 activity of *Trichoderma virens* transformants constitutively coexpressing beta-1,3- and beta-1,6-
432 glucanase genes. *Mol Plant Pathol.* 8, 469-80.

433

434 Druzhinina, I. S., Shelest, E. & Kubicek, C. P. 2012. Novel traits of *Trichoderma* predicted through
435 the analysis of its secretome. *FEMS Microbiol Lett* 337, 1-9.

436

437 Genre, A., Chabaud, M., Timmers, T., Bonfante, P. & Barker, D. G. 2005. Arbuscular mycorrhizal
438 fungi elicit a novel intracellular apparatus in *Medicago truncatula* root epidermal cells before
439 infection. *Plant cell online* 17, 3489.

440

441 Genre, A., Bonfante, P. 2007. Check-in procedures for plant cell entry by biotrophic
442 microbes. *MPMI* 20, 1023-1030.

443

444 Genre, A., Chabaud, M., Faccio, A., Barker, D. G. & Bonfante, P. 2008. Prepenetration apparatus
445 assembly precedes and predicts the colonization patterns of arbuscular mycorrhizal fungi within the

446 root cortex of both *Medicago truncatula* and *Daucus carota*. Plant cell 20, 1407–20.

447

448 Genre, A., Ortu, G., Bertoldo, C., Martino, E. & Bonfante, P. 2009. Biotic and abiotic stimulation
 449 of root epidermal cells reveals common and specific responses to arbuscular mycorrhizal fungi.
 450 Plant physiol. 149, 1424-34.

451

452 Harman, G.E. 2000. Myths and dogmas of biocontrol. Changes in perceptions derived from
 453 research on *Trichoderma harzianum* T22. Plant disease 84, 377–393.

454

455 Harman, G.E., Howell, C.R., Viterbo, A., Chet, I. & Lorito, M. 2004. *Trichoderma* species-
 456 opportunistic, avirulent plant symbionts. Nat Rev Microbiol 2, 43-56.

457

458 Harman, G.E. 2011. Multifunctional fungal plant symbionts: new tools to enhance plant growth and
 459 productivity. New Phytol. 189, 647-9.

460

461 Hoch, H.C. 1986. Freeze-substitution of fungi. In: Aldrich HC, Todd WJ, eds. Ultrastructure
 462 techniques of microorganisms. New York: Plenum Press, 183–211.

463

464 Howard, R.J., O'Donnell, K.L. 1987. Freeze substitution of fungi for cytological analysis. Exp
 465 Mycol. 11, 250– 269.

466

467 Howell, C.R. 2006. Understanding the mechanisms employed by *Trichoderma virens* to effect
 468 biological control of cotton diseases. Phytopathology 96, 178-80.

469

470 Kubicek, C. P. *et al.* 2011. Comparative genome sequence analysis underscores mycoparasitism as
471 the ancestral life style of *Trichoderma*. Genome biol. 12, R40.

472

473 Lorito, M., Harman, G.E., Hayes, C.K., Broadway, R.M., Tronsmo, A., Woo, S.L. and Di Pietro, A.
474 1993a. Chitinolytic enzymes produced by *Trichoderma harzianum*: antifungal activity of purified
475 endochitinase and chitobiosidase. Phytopathology 83, 302-307.

476

477 Lorito, M., Di Pietro, A., Hayes, C.K., Woo, S., Harman, G.E. 1993b. Antifungal, synergistic
478 interaction between chitinolytic enzymes from *Trichoderma harzianum* and *Enterobacter cloacae*.
479 Phytopathology 83, 721-728.

480

481 Lorito M., Hayes, C.K., Di Pietro, A., Woo, S.L. and Harman, G.E. 1994. Purification,
482 characterization and synergistic activity of a glucan 1,3- β -glucosidase and an N-acetyl- β -
483 glucosaminidase from *Trichoderma harzianum*. Phytopathology 84, 398-405.

484

485 Lorito, M., Farkas, V., Rebuffat, S., Bodo, B., Kubicek, C.P. 1996. Cell wall synthesis is a major
486 target of mycoparasitic antagonism by *Trichoderma harzianum*. J Bacteriol. 178, 6382-5.

487

488 Lorito, M., Woo, S.L., Harman, G.E., Monte, E. 2010. Translational research on *Trichoderma*: from
489 genomics to the field. Annu Rev Phytopathol. 48, 395-417.

490

491 Lorito, M, and Woo, S.L. 2014. *Trichoderma*: a multi-purpose tool for IPM, in Principles of Plant-
492 Microbe Interactions, Ed. B. Lugtenberg. Springer (in press).

493

494 Lu, Z., Tombolini, R., Woo, S., Lorito, M., Jansson, J.K., Zeilinger, S. 2004. In vivo study of
 495 *Trichoderma*-pathogen-plant interactions using constitutive and inducible green fluorescent protein
 496 reporter. Appl Environ Microbiol. 70, 3073.
 497
 498 Martinez, D. *et al.* 2008. Genome sequencing and analysis of the biomass-degrading fungus
 499 *Trichoderma reesei* (syn. *Hypocrea jecorina*). Nat biotechnol. 26, 553-60.
 500
 501 Martínez-Medina, A., Roldán, A., Albacete, A. & Pascual, J. 2011. The interaction with arbuscular
 502 mycorrhizal fungi or *Trichoderma harzianum* alters the shoot hormonal profile in melon plants.
 503 Phytochemistry 72, 223–9.
 504
 505 Miyawaki, A., Llopis, J., Heim, R., Mccaffery, J.M., Adams, J.A., Ikurak, M., Tsien, R.Y. 1997.
 506 Fluorescent indicators for Ca^{2+} based on green fluorescent proteins and calmodulin. Nature 388,
 507 882-887.
 508
 509 Miyawaki, A., Griesbeck, O., Heim, R. & Tsien, R.Y. 1999. Dynamic and quantitative Ca^{2+}
 510 measurements using improved cameleons. PNAS 96, 2135-40.
 511
 512 Morán-Diez, E., Rubio, B., Domínguez, S., Hermosa, R., Monte, E., Nicolás, C. 2012.
 513 Transcriptomic response of *Arabidopsis thaliana* after 24 h incubation with the biocontrol fungus
 514 *Trichoderma harzianum*. J Plant Physiol. 169, 614-20.
 515
 516 Navazio, L., Baldan, B., Moscatiello, R., Woo, S.L., Mariani, P., Lorito, M. 2007. Calcium-
 517 mediated perception and defense responses activated in plant cells by metabolite mixtures secreted

518 by the biocontrol fungus *Trichoderma atroviride*. BMC Plant biol 7, 41.

519

520 Palmieri, M.C., Perazzolli, M., Matafora, V., Moretto, M., Bachi, A., Pertot, I. 2012. Proteomic

521 analysis of grapevine resistance induced by *Trichoderma harzianum* T39 reveals specific defence

522 pathways activated against downy mildew. J Exp Bot. 63, 6237-51.

523

524 Perazzolli, M., Moretto, M., Fontana, P., Ferrarini, A., Velasco, R., Moser, C., Delledonne, M. and

525 Pertot, I. 2012. Downy mildew resistance induced by *Trichoderma harzianum* T39 in susceptible

526 grapevines partially mimics transcriptional changes of resistant genotypes. BMC Genomics, 13:

527 660.

528

529 Reynolds, E.W. 1963. The use of lead citrate at high pH as an electron opaque stain in electron

530 microscopy. J Cell Biol 17, 208-212.

531

532 Rousseau, A., Benhamou, N., Chet, I. & Piché Y. 1996. Mycoparasitism of the extramatrical phase

533 of *Glomus intraradices* by *Trichoderma harzianum*. Phytopathology 86, 434–443.

534

535 Schäfer, P., Khatabi, B. & Kogel, K.H. 2007. Root cell death and systemic effects of

536 *Piriformospora indica*: a study on mutualism. FEMS microbiol let. 275, 1–7.

537

538 Schirmböck, M., Lorito, M., Wang, Y.L., Hayes, C.K., Arisan-Atac, I., Scala, F., Harman, G.E.,

539 Kubicek, C.P. 1994. Parallel formation and synergism of hydrolytic enzymes and peptaibol

540 antibiotics, molecular mechanisms involved in the antagonistic action of *Trichoderma harzianum*
 541 against phytopathogenic fungi. Appl Environ Microbiol. 60, 4364-70.

542

543 Séjalon-Delmas, N., Magnier, A., Douds, D.D., Jr., and Bécard, G. 1998. Cytoplasmic
 544 autofluorescence of an arbuscular mycorrhizal fungus *Gigaspora gigantea* and nondestructive
 545 fungal observations in planta. Mycologia 90, 921–926.

546

547 Shores, M., Harman, G.E., Mastouri, F. 2010. Induced systemic resistance and plant responses to
 548 fungal biocontrol agents. Annu Rev Phytopathol. 48, 21-43.

549

550 Sieberer, B.J., Chabaud, M., Timmers, A.C., Monin, A., Fournier, J. and Barker, D.G. 2009. A
 551 nuclear-targetedameleon demonstrates intranuclear Ca^{2+} spiking in *Medicago truncatula* root
 552 hairs in response to rhizobial nodulation factors. Plant physiol 151, 1197-206.

553

554 Singh, S. and Parniske, M. 2012. Activation of calcium- and calmodulin-dependent protein kinase
 555 (CCaMK), the central regulator of plant root endosymbiosis. Curr Opin Plant Biol. 15, 444–453.

556

557 Tisserant, E. *et al.* 2013. Genome of an arbuscular mycorrhizal fungus provides insight into the
 558 oldest plant symbiosis. Proc Natl Acad Sci 110, 20117-22.

559

560 Tucci, M., Ruocco, M., De Masi, L., De Palma, M., Lorito, M. 2011. The beneficial effect of
 561 *Trichoderma spp.* on tomato is modulated by the plant genotype. Mol Plant Pathol. 12, 341-54.

562

563 Vargas, W.A., Mandawe, J.C., Kenerley, C.M. 2009. Plant-derived sucrose is a key element in the

564 symbiotic association between *Trichoderma virens* and maize plants. Plant Physiol. 151, 792-808.

565

566 Woo, S.L., Donzelli, B., Scala, F., Mach, R., Harman, G.E., Kubicek, C.P., Del Sorbo, G. and

567 Lorito, M. 1999. Disruption of the *ech42* (endochitinase-encoding) gene affects biocontrol activity

568 in *Trichoderma harzianum* P1. MPMI 12, 419-429.

569

570 Zeilinger, S., Galhaup, C., Payer, K., Woo, S.L., Mach, R.L., Fekete, C., Lorito, M., and Kubicek,

571 C.P. 1999. Chitinase gene expression during mycoparasitic interaction of *Trichoderma harzianum*

572 with its host. Fungal Genet. Biol. 26, 131-140.

573

574 FIGURE CAPTIONS

575

576 **Figure 1.** Interaction of *Trichoderma atroviride* strain P1 expressing the GFP protein (mutant

577 PKI1) (green) with the autofluorescent AM fungus *Gigaspora gigantea* (red), observed in confocal

578 laser microscopy 24 (A), 48 (B and C) and 72 (D and E) hours post inoculation. A, Contact between

579 hyphae of *T. atroviride* (Ta), and *G. gigantea* (Gg). No specialized adhesion structures are

580 recognizable associated with hyphal contact. B, Images of *G. gigantea* cytoplasmic rupture

581 (asterisk) observed in fluorescence (top) and transmitted light (bottom) microscopy; presumably

582 due to perforation of the hyphal cell wall by *T. atroviride* hyphae. The hypha of PKI1 is visible

583 inside the AM fungal hypha (double arrowhead). Note the cluster of short branches (arrowheads) of

584 PKI1 hyphae developed towards *G. gigantea* cytoplasmic outburst. C, *T. atroviride* (double

585 arrowheads) growing inside a hypha of *G. gigantea* (dotted line), almost devoid of cytoplasm (as

586 indicated by its low fluorescence), observed under fluorescence (top) and transmitted light

587 (bottom). D, Extensive growth of *T. atroviride* mycelium around and inside *G. gigantea* hyphae and

588 auxilliary cells (ac). E, Higher magnification of the area outlined in D, showing *T. atroviride*

589 hyphae (arrowheads) growing inside the cytoplasm of *G. gigantea* hyphae (h) and auxiliary cells
590 (ac). Bars = 25µm

591
592 **Figure 2.** Transmission electron microscopy images of the dual interaction between *Trichoderma*
593 *atroviride* and *Gigaspora gigantea*. A, Direct contact between the two fungal walls (arrow and
594 boxed area). Both *T. atroviride* (Ta) and *G. gigantea* (Gg) hyphae have healthy cytoplasms with
595 easily recognizable organelles: intact nuclei (n), lipid globules (L) and electron dense granules
596 (arrowheads). B, Higher magnification of the area boxed in A, showing the contact between the
597 electron-transparent wall of *T. atroviride* (arrowhead) and the electron-dense wall of *G. gigantea*
598 (arrow) displaying two distinct dark layers. Amorphous masses (double arrowheads) emerge from
599 the outer layer of the AM fungus. C, *G. gigantea* hypha colonized by *T. atroviride*. The AM hyphal
600 wall is partially degraded (arrow and boxed area); cytoplasm is collapsed into a degenerated mass
601 (arrowhead), and the organelles are no longer distinguishable; by contrast, *T. atroviride* hyphae (Ta)
602 appear healthy and active, displaying nuclei (n) and lipid globules (L). D, Higher magnification of
603 the area boxed in C, showing a site of wall damage in *G. gigantea*: the inner electron-dense layer is
604 replaced by a loose fibrillar matrix (arrow). By contrast, the wall external layer and amorphous
605 masses (double arrowhead) are not degraded. Bars = 2 µm (A and C); 1 µm (B and D).

606
607 **Figure 3.** Interaction of *Trichoderma atroviride* PKI (green) with non-viable (UV-treated) hyphae
608 of *Gigaspora margarita* (red), observed in confocal microscopy after inoculation of *T. atroviride*.
609 A, B 48 hpi, *T. atroviride* (green) extensively colonized *G. margarita* (red) with intra-hyphal coils
610 (arrowhead). C Preferential growth of *T. atroviride* inside cytoplasm-filled hyphae of *G. margarita*
611 (arrowhead) observed in fluorescence (right) and transmitted light (left) 72 hpi: a hyphal branch
612 devoid of cytoplasm (asterisk), delimited by a septum (dotted line), is not colonized by *T.*
613 *atroviride*. D-I, Time-lapse series (total duration = 2h20') showing *T. atroviride* growing inside *G.*

614 *margarita* hyphae. D-F, Branching of *T.atroviride* within a *G. margarita* hyphal branch (arrows).
615 H-I. Swelling and outbreak of *T.atroviride* hyphal tip at the apex of the *G. margarita* hypha (double
616 arrowheads). Note the profuse branching of *T. atroviride* (H, arrowheads) inside the parasitized
617 hyphae. Bars = 20µm

618

619 **Figure 4.** Dual interaction of *Trichoderma atroviride* PKI1 constitutively expressing cytoplasmic
620 GFP (green) with root organ cultures of *Medicago truncatula* expressing GFP-HDEL as a marker of
621 the endoplasmic reticulum. All images are obtained in confocal microscopy. A, B, 48 hpi of *T.*
622 *atroviride*, a hypha (arrowhead) is approaching *M. truncatula* root. The intense fluorescence and
623 integrity of the endoplasmic reticulum lace-like network (B) is a clear indicator of plant cell
624 viability. C, D, 72 hpi, hyphae of the rapidly expanding *T. atroviride* mycelium overlap and coil
625 around the root. Several contacts between hyphae and the root epidermis are visible (arrowheads)
626 but no specialized adhesion structure is recognizable. The partial disorganization of the
627 endoplasmic reticulum is evident in D, in the form of isolated patches and spots of GFP
628 fluorescence. E, F, Six days after *T. atroviride* inoculum, most of the contacted epidermal cells are
629 dead, as indicated by the partial to total disruption of the endoplasmic reticulum, and the
630 disappearance or diffusion (arrow) of GFP fluorescence. Some of the hyphae are visible in F,
631 coiling inside an epidermal cell (asterisk) and growing from cell to cell (double arrowhead). The
632 weak red fluorescence of the plant cell walls becomes apparent in these images due to the absence
633 of the bright GFP signal. Bars = 75 µm (A, C, E); 12µm (B, D, F).

634

635 **Figure 5.** Fluorescence resonance energy transfer (FRET) plots representing nuclear Ca^{2+} levels in
636 epidermal cells of *Medicago truncatula* root organ cultures treated with culture filtrates of
637 *Gigaspora margarita* (A), *Trichoderma atroviride* PKI1 (B), or sterile water as control (C). A,
638 Treatment with 10 times concentrated exudate from germinated *Gigaspora margarita* spores elicits

639 intense spiking over the 40-min acquisition period. B, By contrast, no oscillation is visible in the
640 plots from roots exposed to 10 times concentrated *T. atroviride* culture filtrates. C, No Ca^{2+} signals
641 are elicited in control treatments with sterile water.

642

643 **Figure 6.** AM colonization of *Medicago truncatula* GFP-HDEL root organ cultures by *Gigaspora*
644 *gigantea* before the inoculation of *Trichoderma atroviride* PKI1, observed in confocal microscopy.
645 A, *Gigaspora gigantea* hyphopodium (double arrowhead) adhering to the root epidermis. Root cells
646 display a healthy endoplasmic reticulum (note that GFP labelling extends to the nuclear envelope
647 (n). B, Single optical section from the root cortical tissue. Cells colonized by *G. gigantea* hyphae
648 (outlined by dotted lines) have an intact nucleus (n) and endoplasmic reticulum network
649 (arrowhead). C, Optical section from an inner cortical cell hosting an arbuscule (ar), indicative of
650 the active status of the symbiosis. The large nucleus (n) and arbuscule branches are surrounded by
651 the intense GFP signal accumulated in the lumen of the nuclear envelope and ER respectively. Bars
652 = 25µm.

653

654 **Figure 7.** Triple interaction between *Trichoderma atroviride* strain PKI1 and root organ cultures of
655 *Medicago truncatula* previously colonized by *Gigaspora gigantea*. Fluorescent labeling and color
656 coding are the same as in previous Figures. A, 48 hpi of *T. atroviride* (green), the first hyphae
657 approach the root epidermis (arrowhead). Root epidermal cells and hyphae and auxilliary cells (ac)
658 of *G. gigantea* are fully viable, as indicated by their respective green and red fluorescence. B, Detail
659 of a few epidermal cells showing the integrity of their GFP-labelled endoplasmic reticulum. C, The
660 diffuse branching of *T. atroviride* hyphae towards *G. gigantea* (arrowhead) is evident 72 hpi. D, A
661 higher magnification shows *T. atroviride* hyphae coiling around an auxiliary cell of *G. gigantea*
662 (arrow). In the same image, epidermal cells in the vicinity of *T. atroviride* hyphae display a diffuse
663 fluorescence (asterisk) or complete loss of the GFP signal (arrowhead), indicative of endoplasmic

reticulum disruption and cell death. E, 144 hpi, the loss of epidermal cells viability is evident in the entire contact area, as indicated by the disappearance of GFP fluorescence. F, A higher magnification shows several hyphae of *T. atroviride* (arrows) growing inside the auxilliary cells of *G. gigantea*. G, An optical section from the root inner tissues at the same time interval shows that the endoplasmic reticulum structure is also lost in most cortical cells, including one that hosts *T. atroviride* hyphae (arrow). H, A higher magnification of the same spot shows the details of ER remnants in the form of small GFP-labelled puncta (arrowheads) spread in the cell lumen. *T. atroviride* coils inside the lumen of a dead cell (arrow). Bars = 75 μ m (A, B, C, D); 25 μ m (G, H).

Suppl. Figure 1. Confocal microscopy images of *M. truncatula* GFP-HDEL and *G. gigantea* in the absence of *T. atroviride*. The pictures in A, C and E were recorded at the time of *T. atroviride* inoculation in the corresponding triple cultures (0 hpi), while the images shown in B, D and F correspond to the end point of the experiment (144 hpi). A, B, *Gigaspora gigantea* extraradical hyphae and auxiliary cells (ac) display a strong cytoplasmic fluorescence. C, D, *M. truncatula* root epidermal cells from an axenic culture display undamaged nuclei (arrowheads) and GFP-tagged endoplasmic reticulum, indicative of cell health. E, *G. gigantea* hyphopodium (arrow) adhesion to the root epidermis does not affect cell viability, as confirmed by endoplasmic reticulum integrity. F, Optical section from an inner cortical cell hosting an arbuscule (ar): the full arbuscule development and the integrity of the ER and nucleus (n) provide evidence of the root active symbiotic status and cell viability. Bars = 75 μ m (A, C, E); 25 μ m (B, D, F).

Suppl. Figure 2. Transmission electron microscopy images of chitin labeling with gold-wheat-germ agglutinin in the walls of *Trichoderma atroviride* and *Gigaspora gigantea*. A, *T. atroviride* (Ta, green) hyphae both in direct contact and inside *G. gigantea* (Gg, red). A strong chitin labelling is evident in the walls of both fungi. B, Magnification of *G. gigantea* wall reveals widespread gold

689 granules. Amorphous extrusions (arrowheads) are not labelled. C, Detail of *G. gigantea* wall grown
690 in the absence of *T. atroviride* shows a comparable distribution of gold granules. D, Quantitative
691 analysis of chitin labeling in *G. gigantea* walls in the presence (green) and absence (red) of *T.*
692 *atroviride* colonization. Bars represent the average number of gold granules per square μm . Non
693 parametric Kruskal-Wallis test for the analysis of variance (letters) indicated that the average values
694 are not significantly different. Bars = 0,5 μm

695
696
697 **Suppl. Figure 3.** Fluorescence mean intensity in *T. atroviride ech42::gfp* strain (A) and *nag1::gfp*
698 strain (B) grown in axenic conditions or dual culture with *G. gigantea*. The two strains express
699 cytoplasmic GFP as a reporter of ECH42 (endochitinase) and NAG1 (N-acetylglucosaminidase)
700 gene expression, respectively. Blue = axenic culture; red = dual culture 24 hpi (no hyphal contact),
701 green = dual culture 96 hpi (extensive contact and mycoparasitism). Non parametric Kruskal-Wallis
702 test for the analysis of variance revealed the absence of significant changes in the expression level
703 of ECH42 during the whole time-course of the experiment. NAG1 expression level was weakly
704 enhanced 24 hpi and then decreased to values lower than the axenic culture.

705
706
707 **Suppl. Figure 4.** Movie from a confocal microscope observation of *Gigaspora margarita* hyphae
708 before exposure to UV irradiation. Viability of *G. margarita* hyphae is validated by the presence of
709 strong cytoplasmic streams. Real-time duration = 1 min. Bars = 20 μm .

710
711
712 **Suppl. Figure 5.** Movie from a confocal microscope observation of *Gigaspora margarita* hyphae

713 after 1h30min exposure to UV irradiation. Non-viability of *G. margarita* hyphae is attested by the
714 interruption of cytoplasmic streams. Real-time duration = 1 min. Bars = 20 μ m.

715
716 **Suppl. Figure 6.** Movie from confocal microscope observation of the dual interaction between
717 *Trichoderma atroviride* PKI1 (green) with the non-viable autofluorescent AM fungus *Gigaspora*
718 *margarita* (orange) 72hpi of *T. atroviride*. *Trichoderma* hypha proceeds all along a *Gigaspora*
719 hypha and branches in correspondence of the parasitized hyphal branches. Subsequent profuse
720 branching lead to the occupation of most of the hyphal lumen The swelling of *Trichoderma* hyphal
721 tip was evident as it reached the apex of the *Gigaspora* hypha. Eventually, *Trichoderma* exited the
722 *G. margarita* apex by perforating its terminal wall. Frames were recorded every 10 minutes.

723

724

725

726

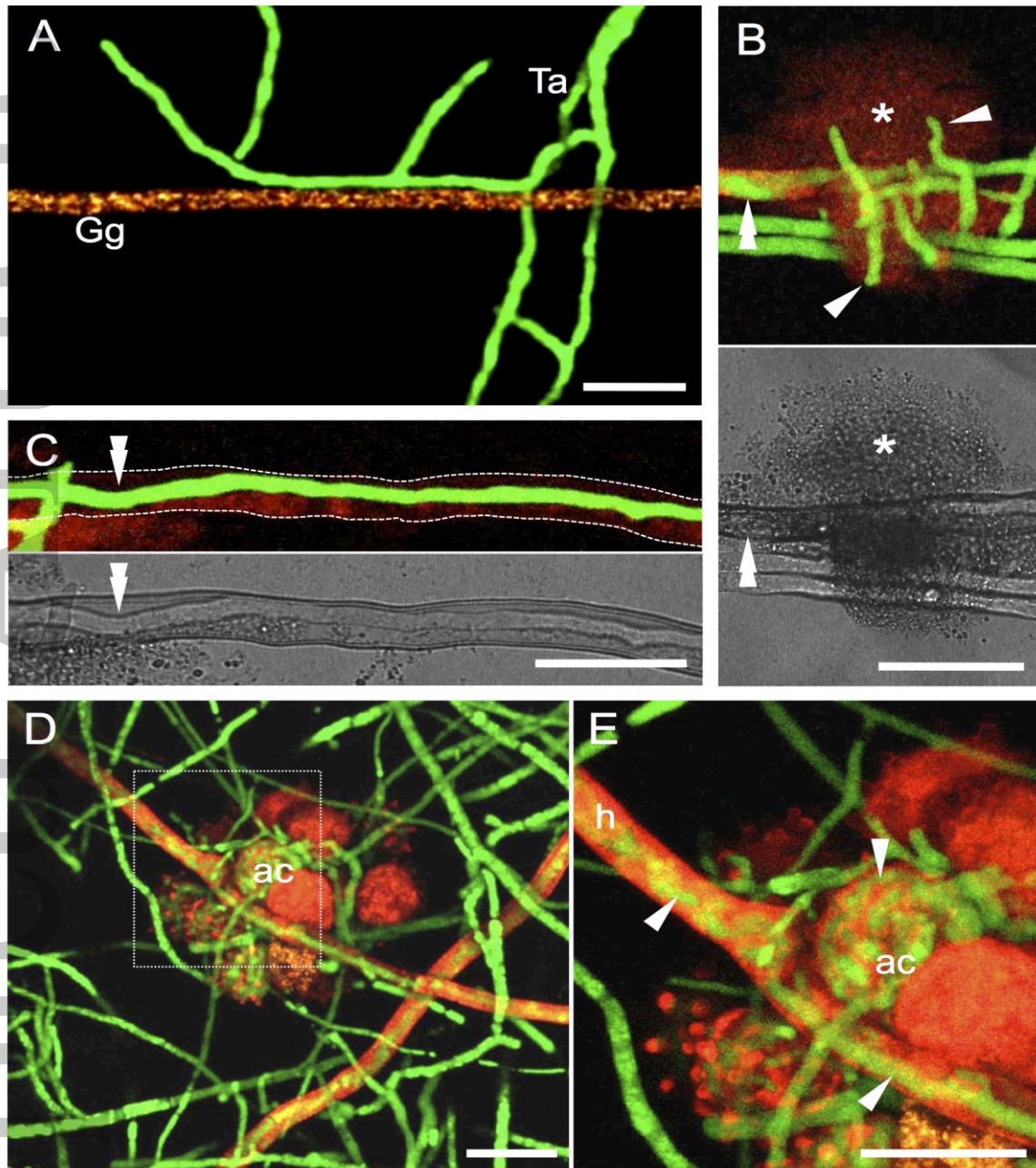


Figure 1. Interaction of *Trichoderma atroviride* strain P1 expressing the GFP protein (mutant PKI1) (green) with the autofluorescent AM fungus *Gigaspora gigantea* (red), observed in confocal laser microscopy 24 (A), 48 (B and C) and 72 (D and E) hours post inoculation. A, Contact between hyphae of *T. atroviride* (Ta), and *G. gigantea* (Gg). No specialized adhesion structures are recognizable associated with hyphal contact. B, Images of *G. gigantea* cytoplasmic rupture (asterisk) observed in fluorescence (top) and transmitted light (bottom) microscopy; presumably due to perforation of the hyphal cell wall by *T. atroviride* hyphae. The hypha of PKI1 is visible inside the AM fungal hypha (double arrowhead). Note the cluster of short branches (arrowheads) of PKI1 hyphae developed towards *G. gigantea* cytoplasmic outburst. C, *T. atroviride* (double arrowheads) growing inside a hypha of *G. gigantea* (dotted line), almost devoid of cytoplasm (as indicated by its low fluorescence), observed under fluorescence (top) and transmitted light (bottom). D, Extensive growth of *T. atroviride* mycelium around and inside *G. gigantea* hyphae and auxiliary cells (ac). E, Higher magnification of the area outlined in D, showing *T. atroviride* hyphae (arrowheads) growing inside the cytoplasm of *G. gigantea* hyphae (h) and auxiliary cells (ac). Bars = 25 μm

EMI4_12221_F1

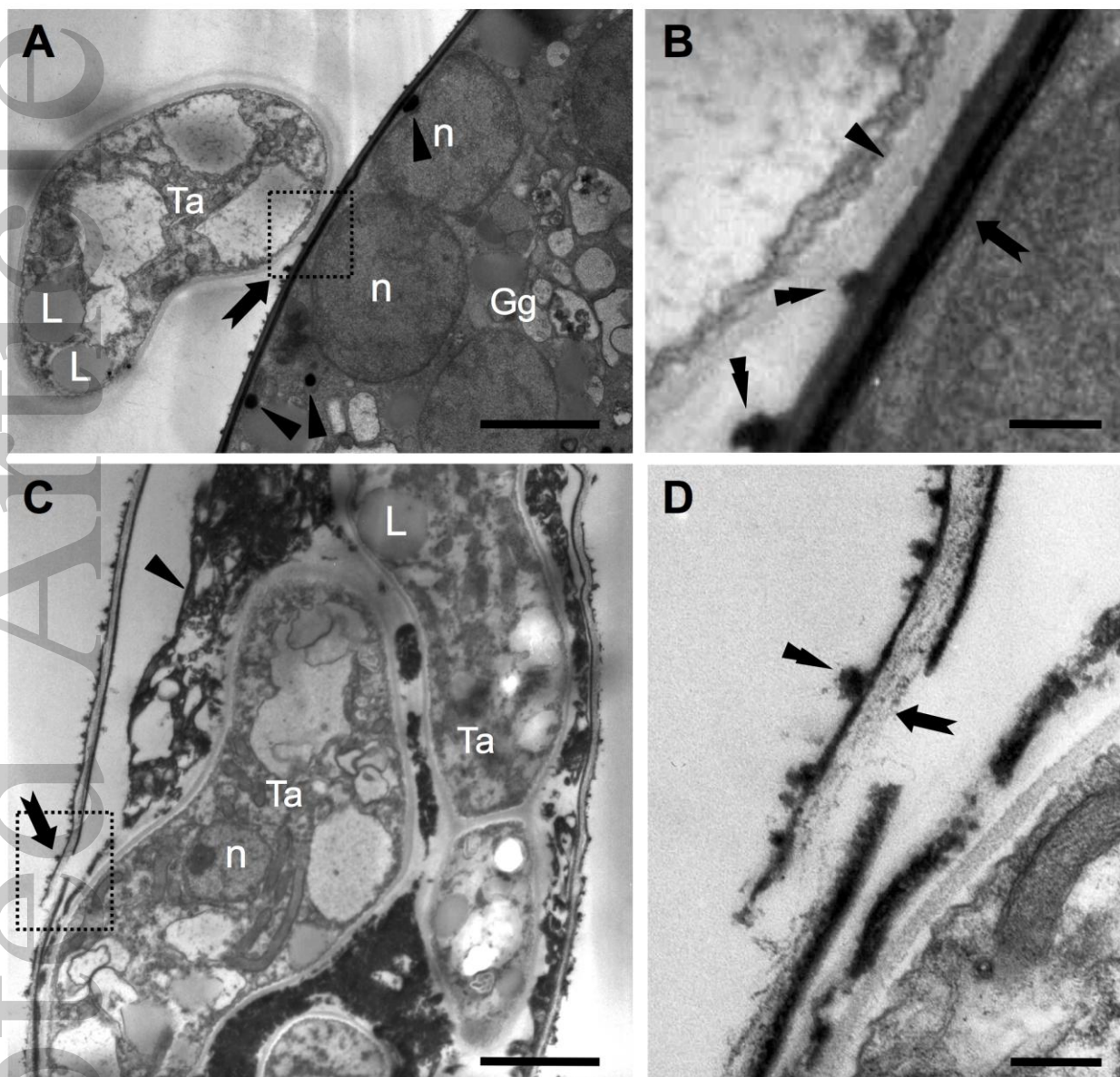


Figure 2. Transmission electron microscopy images of the dual interaction between *Trichoderma atroviride* and *Gigaspora gigantea*. A, Direct contact between the two fungal walls (arrow and boxed area). Both *T. atroviride* (Ta) and *G. gigantea* (Gg) hyphae have healthy cytoplasms with easily recognizable organelles: intact nuclei (n), lipid globules (L) and electron dense granules (arrowheads). B, Higher magnification of the area boxed in A, showing the contact between the electron-transparent wall of *T. atroviride* (arrowhead) and the electron-dense wall of *G. gigantea* (arrow) displaying two distinct dark layers. Amorphous masses (double arrowheads) emerge from the outer layer of the AM fungus. C, *G. gigantea* hypha colonized by *T. atroviride*. The AM hyphal wall is partially degraded (arrow and boxed area); cytoplasm is collapsed into a degenerated mass (arrowhead), and the organelles are no longer distinguishable; by contrast, *T. atroviride* hyphae (Ta) appear healthy and active, displaying nuclei (n) and lipid globules (L). D, Higher magnification of the area boxed in C, showing a site of wall damage in *G. gigantea*: the inner electron-dense layer is replaced by a loose fibrillar matrix (arrow). By contrast, the wall external layer and amorphous masses (double arrowhead) are not degraded. Bars = 2 μ m (A and C); 1 μ m (B and D).

EMI4_12221_F2

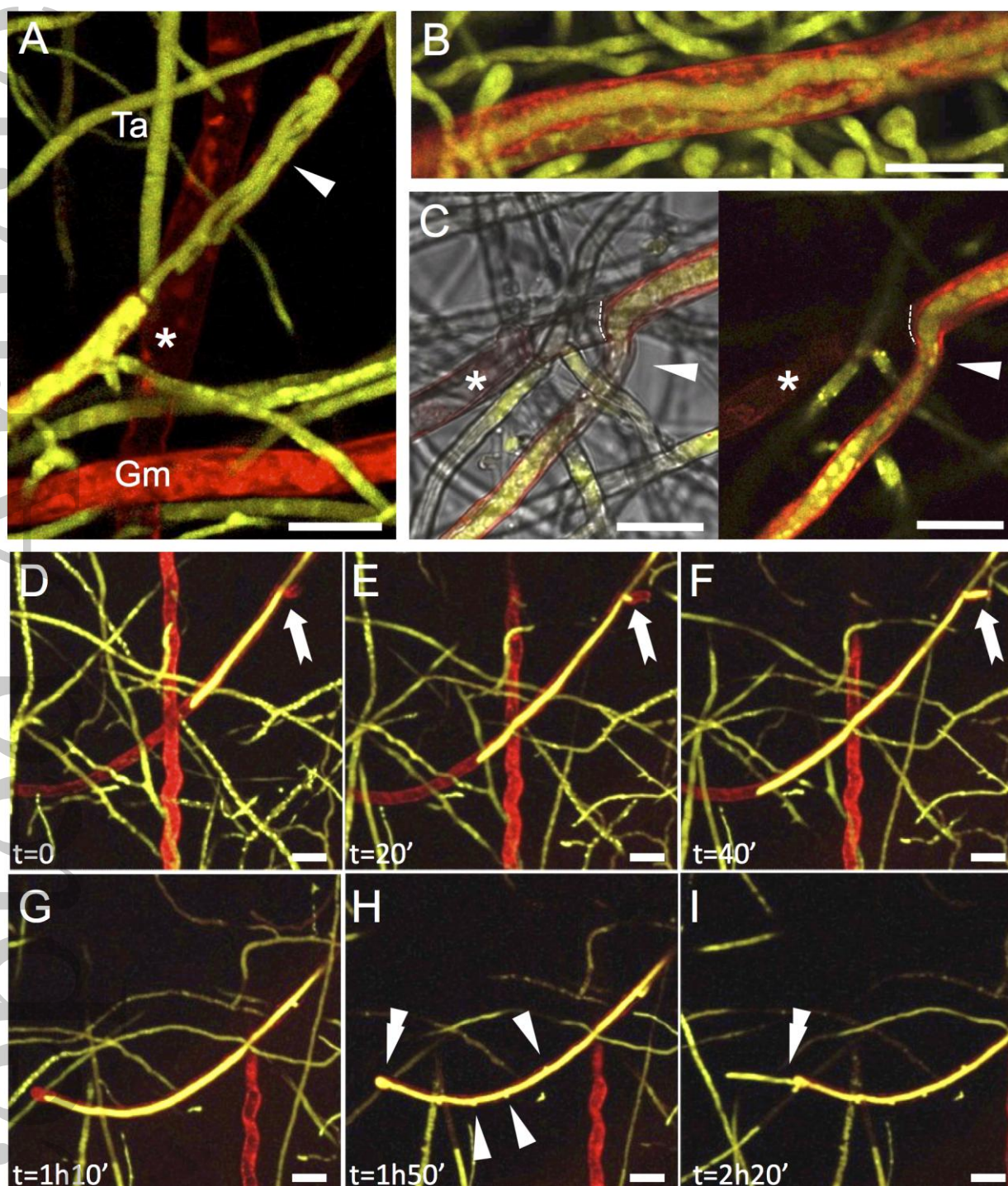


Figure 3. Interaction of *Trichoderma atroviride* PKI (green) with non-viable (UV-treated) hyphae of *Gigaspora margarita* (red), observed in confocal microscopy after inoculation of *T. atroviride*. A, B 48 hpi, *T. atroviride* (green) extensively colonized *G. margarita* (red) with intra-hyphal coils (arrowhead). C Preferential growth of *T. atroviride* inside cytoplasm-filled hyphae of *G. margarita* (arrowhead) observed in fluorescence (right) and transmitted light (left) 72 hpi: a hyphal branch devoid of cytoplasm (asterisk), delimited by a septum (dotted line), is not colonized by *T. atroviride*. D-I, Time-lapse series (total duration = 2h20') showing *T. atroviride* growing inside *G. margarita* hyphae. D-F, Branching of *T. atroviride* within a *G. margarita* hyphal branch. H-I, Swelling and outbreak of *T. atroviride* hyphal tip at the apex of the *G. margarita* hypha (double arrowhead). Note the profuse branching of *T. atroviride* (H, arrowheads) inside the parasitized hyphae. Bars = 20µm

733

734

EMI4_12221_F3

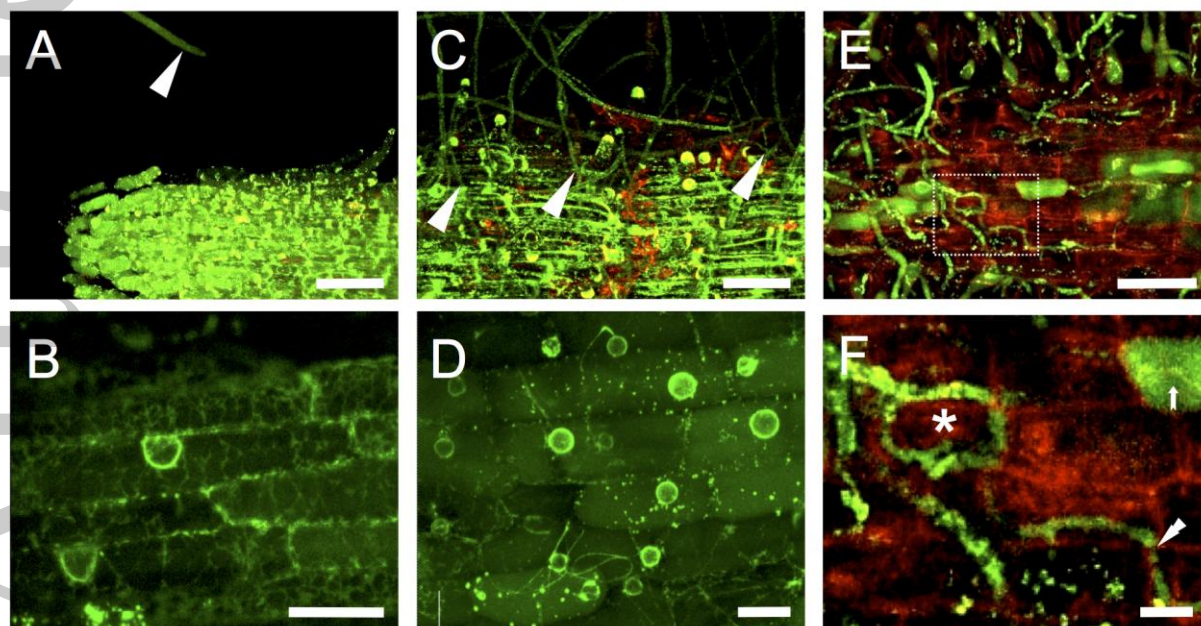


Figure 4. Dual interaction of *Trichoderma atroviride* PKI1 constitutively expressing cytoplasmic GFP (green) with root organ cultures of *Medicago truncatula* expressing GFP-HDEL as a marker of the endoplasmic reticulum. All images are obtained in confocal microscopy. A, B, 48 hpi of *T. atroviride*, a hypha (arrowhead) is approaching *M. truncatula* root. The intense fluorescence and integrity of the endoplasmic reticulum lace-like network (B) is a clear indicator of plant cell viability. C, D, 72 hpi, hyphae of the rapidly expanding *T. atroviride* mycelium overlap and coil around the root. Several contacts between hyphae and the root epidermis are visible (arrowheads) but no specialized adhesion structure is recognizable. The partial disorganization of the endoplasmic reticulum is evident in D, in the form of isolated patches and spots of GFP fluorescence. E, F, Six days after *T. atroviride* inoculum, most of the contacted epidermal cells are dead, as indicated by the partial to total disruption of the endoplasmic reticulum, and the disappearance or diffusion (arrow) of GFP fluorescence. Some of the hyphae are visible in F, coiling inside an epidermal cell (asterisk) and growing from cell to cell (double arrowhead). The weak red fluorescence of the plant cell walls becomes apparent in these images due to the absence of the bright GFP signal. Bars = 75 μ m (A, C, E); 12 μ m (B, D, F).

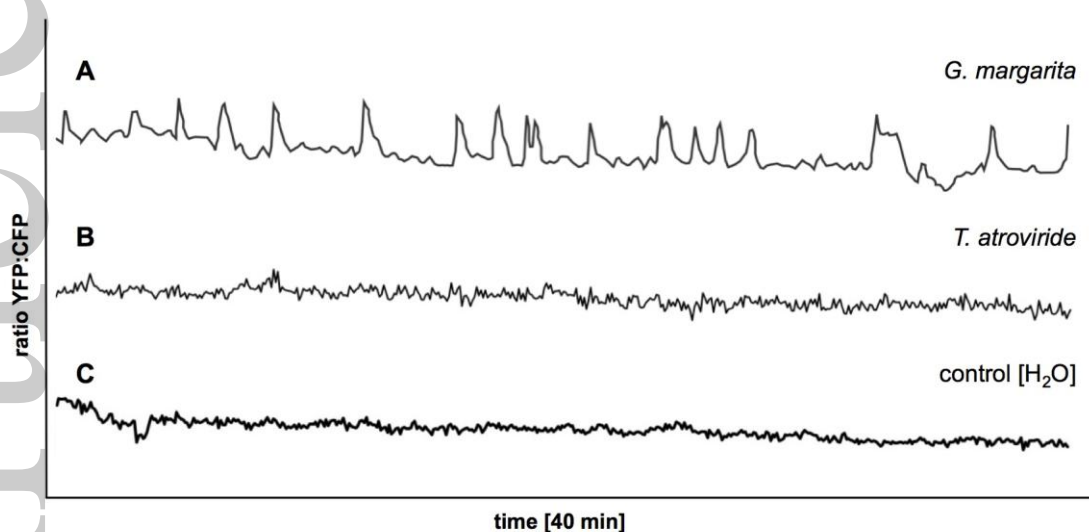


Figure 5. Fluorescence resonance energy transfer (FRET) plots representing nuclear Ca^{2+} levels in epidermal cells of *Medicago truncatula* root organ cultures treated with culture filtrates of *Gigaspora margarita* (A), *Trichoderma atroviride* PK11 (B), or sterile water as control (C). A, Treatment with 10 times concentrated exudate from germinated *Gigaspora margarita* spores elicits intense spiking over the 40-min acquisition period. B, By contrast, no oscillation is visible in the plots from roots exposed to 10 times concentrated *T. atroviride* culture filtrates. C, No Ca^{2+} signals are elicited in control treatments with sterile water.

EMI4_12221_F5

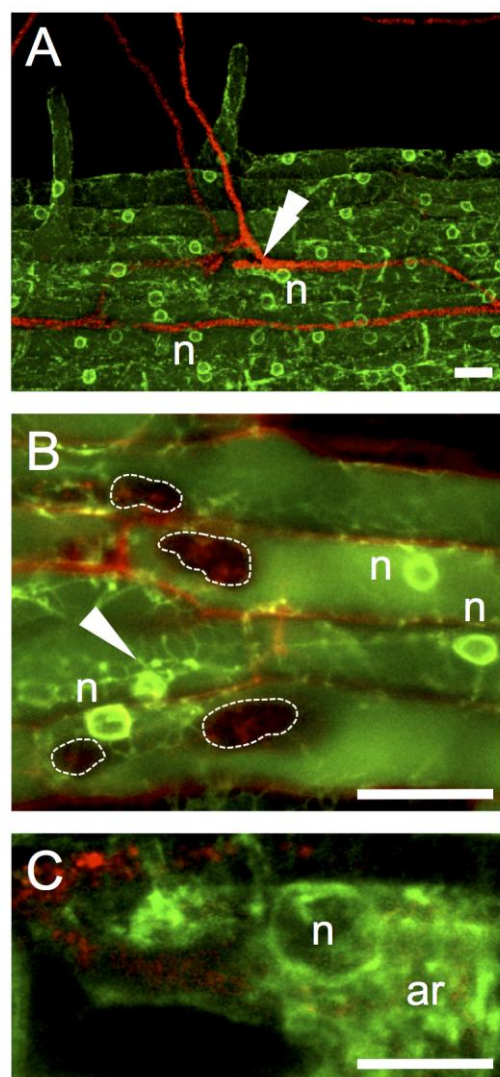
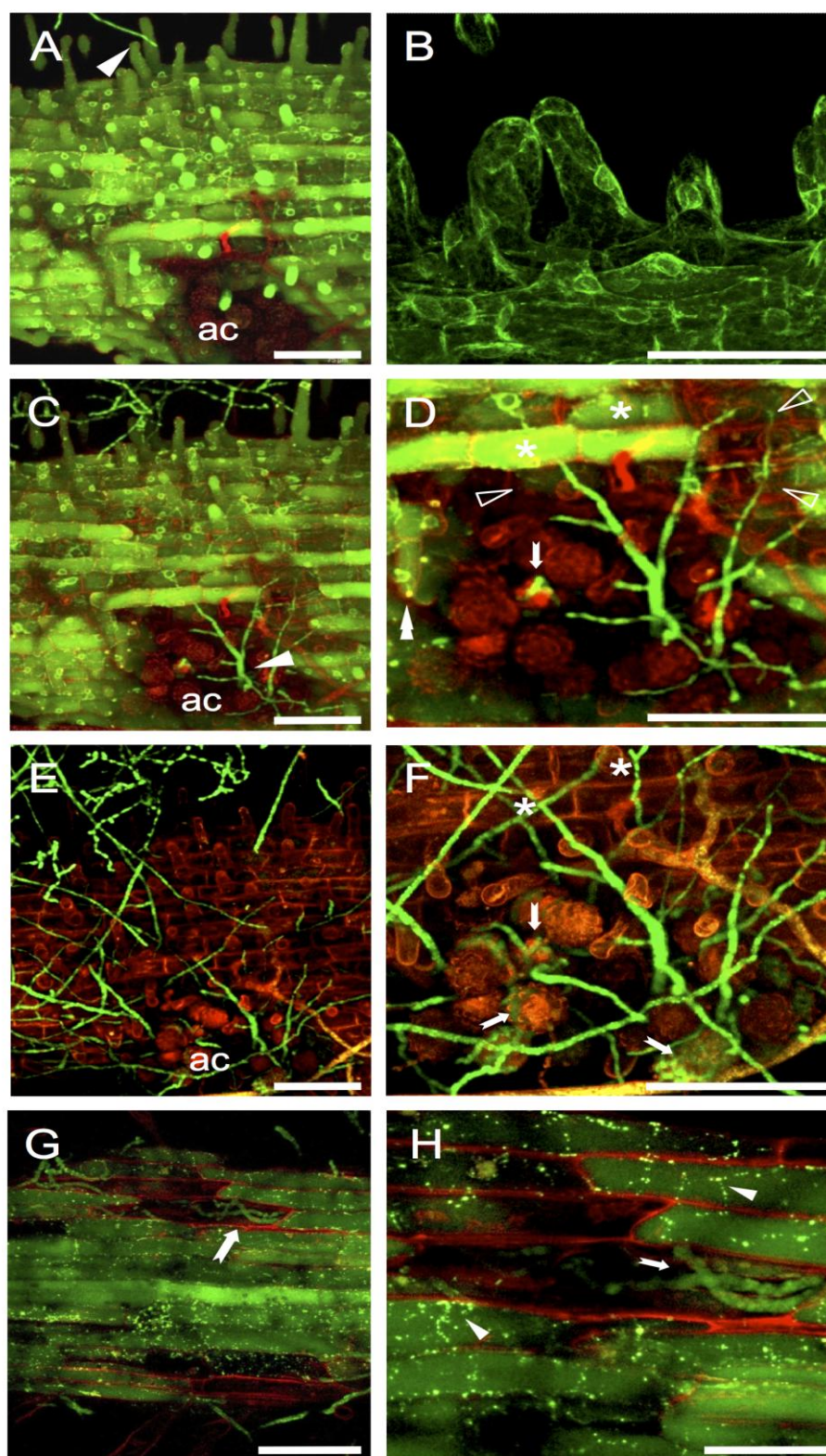


Figure 6. AM colonization of *Medicago truncatula* GFP-HDEL root organ cultures by *Gigaspora gigantea* before the inoculation of *Trichoderma atroviride* PKI1, observed in confocal microscopy. A, *Gigaspora gigantea* hyphopodium (double arrowhead) adhering to the root epidermis. Root cells display a healthy endoplasmic reticulum (note that GFP labelling extends to the nuclear envelope (n)). B, Single optical section from the root cortical tissue. Cells colonized by *G. gigantea* hyphae (outlined by dotted lines) have an intact nucleus (n) and endoplasmic reticulum network (arrowhead). C, Optical section from an inner cortical cell hosting an arbuscule (ar), indicative of the active status of the symbiosis. The large nucleus (n) and arbuscule branches are surrounded by the intense GFP signal accumulated in the lumen of the nuclear envelope and ER respectively. Bars = 25µm.

EMI4_12221_F6



EMI4_12221_F7